PHYSICAL REVIEW B **79**, 140403(R) (2009)

Universality of the surface magnetoelectric effect in half-metals

Chun-Gang Duan,[1,*] Ce-Wen Nan,[2] S. S. Jaswal,[3] and E. Y. Tsymbal[3,†]

[1]*Key Laboratory of Polar Materials and Devices, Ministry of Education, East China Normal University, Shanghai 200062, China*

[2]*Department of Materials Science and Engineering, State Key Laboratory of New Ceramics and Fine Processing, Tsinghua University, Beijing 100084, China*

[3]*Department of Physics and Astronomy, Nebraska Center for Materials and Nanoscience, University of Nebraska, Lincoln, Nebraska 68588, USA*

(Received 3 March 2009; published 7 April 2009)

An electric field applied to a ferromagnetic metal produces a surface magnetoelectric effect originating from the spin-dependent screening of the electric field which results in a change in the surface magnetization of the ferromagnet. Here we predict that if the ferromagnet is a half-metal, due to the screening charge formed solely by single-spin conducting states, the surface magnetoelectric coefficient is the universal constant $\mu_B/ec^2 \approx 6.44\times10^{-14}$ G cm^2/V. This prediction is in excellent agreement with results of our first-principles calculations of the magnetic response of a half-metallic CrO_2 to an applied electric field. The universal value of the surface magnetoelectric coefficient in half-metals may be used as another tool for detecting half-metallicity.

DOI: 10.1103/PhysRevB.79.140403 PACS number(s): 75.80.+q, 75.70.Ak, 77.84.−s, 75.75.+a

Magnetoelectric materials have recently stimulated a surge of research activities in material science.[1–3] An important property making these materials attractive is the *magnetoelectric effect*, i.e., the induction of magnetization by an electric field or electric polarization by a magnetic field. In a broader vision, magnetoelectric effects include not only the coupling between the order parameters[1] but also involve related phenomena such as electrically controlled magnetocrystalline anisotropy,[4–8] exchange bias,[9,10] and spin transport.[11–17] Tailoring the magnetization, magnetic anisotropy, exchange bias, and spin transport by electric fields opens unexplored avenues for device applications.

There are several mechanisms responsible for the magnetoelectric effect. An intrinsic magnetoelectric coupling occurs in compounds with no time-reversal and no space-inversion symmetries.[18] In such materials, an external electric field displaces the magnetic ions, eventually changing the exchange interactions between them and hence the magnetic properties of the compound.[19] A different mechanism of magnetoelectric coupling may occur in composites of piezoelectric (ferroelectric) and magnetostrictive (ferromagnetic or ferrimagnetic) compounds. In such structures, an applied electric field induces strain in the piezoelectric constituent which is mechanically transferred to the magnetostrictive constituent, where it induces a magnetization.[20] In recent years, composite multiferroics have been intensively studied.[21–25] The importance of composite multiferroics follows from the fact that none of the existing single phase multiferroic materials combine large and robust electric and magnetic polarizations at room temperature[1–3]

In addition to the strain, the magnetoelectric effect that occurs at the ferromagnet/insulator interface may have purely electronic origin. Duan *et al.*[26] predicted that atomic displacements at the $Fe/BaTiO_3(001)$ interface caused by ferroelectric switching change the overlap between atomic orbitals at the interface that affects the interface magnetization. A similar effect was found by Yamauchi *et al.*[27] for the $Co_2MnSi/BaTiO_3(001)$ interface and Niranjan *et al.*[28] for the $Fe_3O_4/BaTiO_3(001)$ interface. Recently Rondinelli *et al.*[29] predicted that the magnetoelectric effect at the $SrRuO_3/SrTiO_3$ interface may be mediated by free carriers. In this case, an electric field results in the accumulation of spin-polarized electrons or holes at the metal-insulator interface producing a change in the interface magnetization. The latter mechanism may be considered as a consequence of spin-dependent screening of an electric field, as was predicted by Zhang.[30] Very recently, we explored the surface magnetoelectric effect due to the direct influence of an external electric field on magnetic properties of ferromagnetic metal films.[31] We found that the spin-dependent screening leads to the spin imbalance of the excess surface charge, resulting in notable changes in the surface magnetization and the surface magnetocrystalline anisotropy.

In this Rapid Communication we show that the magnetoelectric coefficient for all half-metallic surfaces is a universal constant. Half-metals are ferromagnetic materials in which one spin band has a gap around the Fermi energy.[32,33] This implies that conducting electrons are present only in one spin channel and the other spin channel is insulating, as is shown schematically in Fig. 1. Due to this feature, the screening of an applied electric field in half-metals is produced solely by carriers (electrons or holes) of the certain spin character. This leads to the induced magnetic moment being proportional to the amount of the screening charge which makes the magnetoelectric coefficient a universal constant independent of the type of half-metal. This property of half-metals is different from ordinary ferromagnetic metals where the screening charge is distributed between majority- and minority-spin states and the surface magnetoelectric coefficient is a fraction of this constant. This unique feature of the surface magnetoelectric effect in half-metals may be used to detect half-metallicity at the surface.

The universal value of the surface magnetoelectric coefficient in half-metals can be seen from the following simple analysis. By definition, the surface magnetization change ΔM due to the applied electric field E is determined by the surface magnetoelectric coefficient α_S according to Ref. 31,

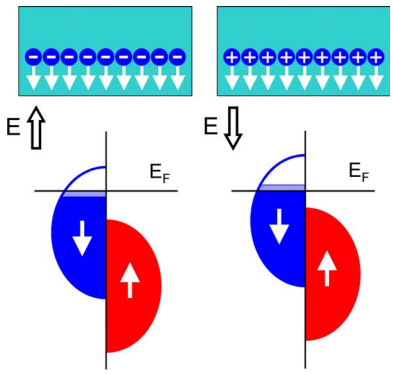

FIG. 1. (Color online) Schematic of the surface magnetoelectric effect in half-metals. Bottom panels show schematically a spin-dependent local density of states at the surface of a half-metal and a change in electron occupation (shaded areas) due to external electric field pointing toward (left panel) and away from (right panel) the surface of a half-metal. The electron occupation change comes entirely from the down-spin states available at the Fermi energy (E_F). Top panels show the respective accumulation of down-spin charge carriers at the half-metal surface. Here negative screening charges are electrons and positive screening charges are holes.

$$\mu_0 \Delta M = \alpha_S E. \tag{1}$$

Here a positive electric field is defined to be pointed away from the metal surface. The change in the magnetization is determined by the screening surface charge $\sigma = \varepsilon_0 E$, where ε_0 is the electric permittivity of vacuum. The screening charge is distributed over the screening length, characterizing the penetration of the external electric field into the metal, which is typically of the order of 1 Å. We note that the screening charge is very small compared to the valence charge in the system. For an applied electric field as strong as 1 V/Å, the screening charge is only about $0.005e/\text{Å}^2$. Such a small screening charge does not affect main features of the electronic structure of the metal and only slightly changes populations of electronic states.

In case of a half-metal, screening occurs entirely through the single conducting spin channel, as is illustrated in Fig. 1. The change in magnetization per unit surface area is then $\Delta M = \pm \mu_B \sigma / e = (\pm \varepsilon_0 \mu_B / e) E$, where μ_B is the Bohr magneton, e is the absolute value of the electron charge, and positive (negative) sign corresponds to the conducting minority- (majority-) spin state. Comparing with Eq. (1), we find that the surface magnetoelectric coefficient is given by the universal constant

$$\alpha_S = \pm \frac{\mu_B}{ec^2} \approx \pm 6.44 \times 10^{-14} \frac{\text{G cm}^2}{\text{V}}. \tag{2}$$

The above result is astonishing since it indicates that the surface magnetoelectric coefficient of half-metals is independent of their chemical constituents and details of their atomic and electronic structure. As long as the surface of a half-metal preserves its half-metallicity, the α_S is given by Eq. (2). We note that the results obtained with free-electron model[30] and a simple rigid-band model[31] reduce to Eq. (2) for half-metals. However, the derivation of Eq. (2) in this Rapid Communication involves neither any approximations regarding the electronic structure nor the mechanism of screening and hence for half-metals is more general.

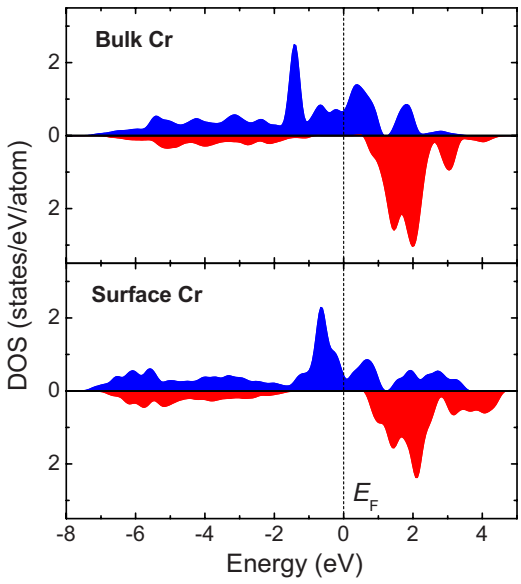

FIG. 2. (Color online) Spin-polarized density of states at the bulk and surface Cr atoms in a 15-monolayer (22-Å-thick) CrO_2 (001) film. Top (bottom) panels show majority(minority)-spin DOS. The vertical line denotes the Fermi energy (E_F).

In order to check this prediction for a realistic half-metal by taking into account explicitly its electronic band structure, we carry out density-functional calculations of the magnetoelectric effect at the (001) surface of chromium dioxide. CrO_2 is predicted to be a half-metal in the bulk[34] which is consistent with experimental observations.[35] It was also found that CrO_2 maintains its half-metallicity at the (001) surface,[36] which is important for the phenomenon addressed in this Rapid Communication.

Our calculations are based on the projector augmented wave (PAW) method implemented in the Vienna *ab initio* simulation package (VASP).[37,38]We consider a free-standing ferromagnetic films of CrO_2(001) under the influence of a uniform electric field applied perpendicular to the film surface. The external electric field is introduced by planar dipole layer method.[39]

Bulk CrO_2 has a tetragonal rutile structure with the lattice parameters $a = 4.42$ Å and $c = 2.92$ Å. In the film geometry, we assume that the two surfaces of the slab are identical, so that the CrO_2 slab is nonstoichiometric. With film thickness ranging from about 10 to 22 Å, all the CrO_2 films studied show half-metallicity for relaxed and unrelaxed configurations. This is consistent with previous theoretical studies.[40] Figure 2 shows the calculated spin-polarized density of states (DOS) of a 15-monolayer (22-Å-thick) CrO_2 film. As seen from the figure, both bulk and surface DOS at the Cr atom display half-metallicity. The latter is evident from only majority-spin states available at the Fermi energy (E_F), minority-spin states exhibiting a band gap around E_F. This behavior is due to the hybridization of the O $2p$ states with the Cr $3d$ states and a large exchange splitting. The latter places the majority $3d$ states at much lower energy, so that

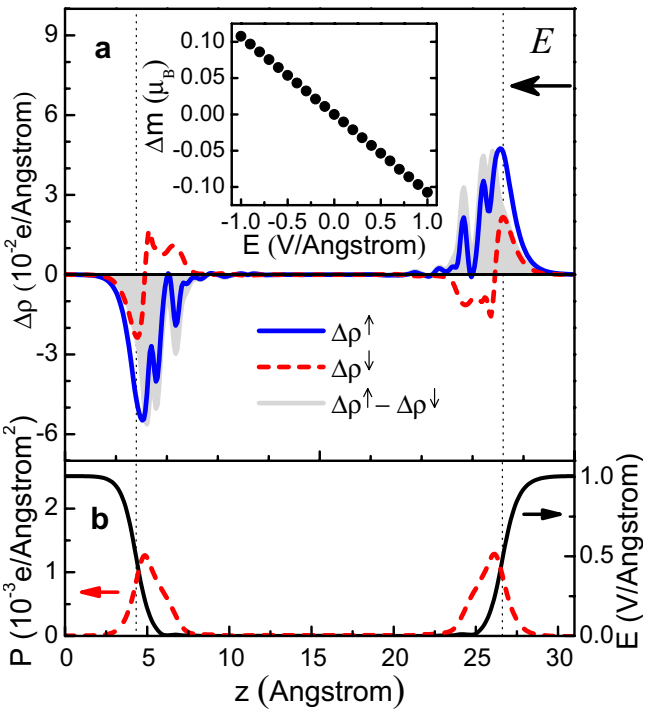

FIG. 3. (Color online) Effects of electric field on electronic properties of a 22-Å-thick CrO_2 (001) film along the z direction normal to the film surface. (a) Induced spin-dependent charge densities $\Delta\rho=\rho(E)-\rho(0)$ for majority-(↑) and minority-(↓) spin electrons and spin density $\Delta\rho^{\uparrow}-\Delta\rho^{\downarrow}$ averaged over the film plane per unit cell area $A=19.55$ Å^2. Inset: induced magnetic moment Δm per unit cell area of the CrO_2 (001) surface as a function of the applied electric field. (b) Variation in the electric field (solid line) and the induced minority-spin polarization (dashed line) across the film. The applied external electric field is $E=1.0$ V/ Å, pointing from right to left. The vertical lines show schematically the two surfaces of the CrO_2 film.

only the majority $3d$ states are partly occupied, i.e., metallic, while the minority $3d$ states are empty, i.e., insulating (see Fig. 2). Two d electrons that are available for the Cr^{4+} ion in CrO_2 occupy majority-spin states yielding an integer magnetic moment of $2\mu_B$/f.u., in agreement with experiments and previous theoretical calculations.

Under the influence of external electric field, the conduction electrons are moved toward or away from the surfaces (depending on the orientation of the field with respect to the surface) to screen the electric field. This leads to the screening charge density of opposite sign localized in the vicinity of the surfaces, as seen from Fig. 3(a). At the distance of about 2 Å from the surfaces, the electric field is fully screened by this charge [see the solid line in Fig. 3(b)].

The important feature of the half-metallic CrO_2 is that the screening occurs entirely due to electrons (holes) in the conducting majority-spin channel [the solid line in Fig. 3(a)]. The minority-spin electrons respond to the electric field as bound electrons in a dielectric. This is seen from the minority-spin charge density $\Delta\rho^{\downarrow}$ [the dashed line in Fig. 3(a)] that reveals electric dipoles at the two surfaces with the net-induced minority-spin charge at each surface being zero. The dashed line in Fig. 3(b) shows the electric polarization **P**, corresponding to the accumulated minority-spin charge density. The polarization is calculated by integrating equation $\Delta\rho^{\downarrow}=-\nabla\cdot\mathbf{P}$ and reflects the response of minority-spin electrons to the electric field shown by the solid line in Fig. 3(b). It is seen from Fig. 3(b) that **P** is nonzero only near the surfaces of the film and is oriented in the direction of the field.

The consequence of spin-dependent screening is an excess spin density of opposite sign formed at the two interfaces [the shaded area in Fig. 3(a)], which implies an electrically induced surface magnetization. As seen from the inset of Fig. 3(a), the magnetic moment per unit cell area changes linearly with electric field. The negative slope of the curve reflects the presence of holes (electrons) in the conducting majority-spin states when the field is pointing away from (toward) the surface. The slope of this curve determines the surface magnetoelectric coefficient $\alpha_S\approx-6.41\times10^{-14}$ G cm^2/V. Remarkably, within the computation error,[41] this value is identical to that given by Eq. (2). The latter result is independent of film thickness (as long as it is larger then the screening length) and atomic relaxations (as long as the film exhibits full half-metallicity). Thus, our density-functional calculations confirm the prediction of the universal magnetoelectric coefficient of half-metals.

We note that the universal value of the magnetoelectric coefficient is applicable to systems where the orbital contribution to the surface magnetic moment is negligibly small. For the CrO_2 (001) surface, we find the orbital magnetic moment is $m_L=-0.021\,7\mu_B$ at zero electric field and $m_L=-0.021\,1\mu_B$ at $E=1$ V/Å. This implies a contribution to the magnetoelectric coefficient of a fraction of 1%. However, a large orbital magnetic moment in a half-metal could make a non-negligible contribution to the magnetoelectric coefficient, thereby producing a departure from the universal behavior.

The universal value of the magnetoelectric coefficient in half-metals may be used as another tool to detect half-metallicity. It is known that not all half-metals preserve half-metallicity on their surfaces. However, half-metallicity at the surface found through the magnetoelectric coefficient would be a strong indication that the bulk is also half-metallic. Although this is a challenging experimental problem due to a relatively small value of the magnetoelectric coefficient, recent advances in surface-sensitive techniques, such as magnetic circular dichroism (MCD), and in particular MCD using the transmission electron microscope[42] allow measuring magnetic moments with unprecedented accuracy and spatial resolution. We therefore hope that such or similar experimental techniques will make it possible to observe the predicted effect.

In conclusion, we have predicted that the surface magnetoelectric coefficient of half-metals is a universal constant, independent of the specifics of atomic and electronic structure, as long as the orbital contribution to the surface magnetic moment can be neglected. Our density-functional calculations applied to CrO_2 (001) surface validate this prediction. The universal value of the surface magnetoelectric coefficient in half-metals may be used as another approach for detecting half-metallicity.

The authors thank Shufeng Zhang for stimulating discussions. This work was supported by the NSF of China (Grant No. 50771072 and No. 50832003), Shanghai Pujiang and ShuGuang Program, Shanghai Leading Academic Discipline Project (Grant No. B411), the Nebraska Research Initiative, the Nanoelectronics Research Initiative of Semiconductor Research Corporation, and Materials Research Science and Engineering Center at the University of Nebraska (Grant No. DMR-0820521).

*wxbdcg@gmail.com

†tsymbal@unl.edu

[1] M. Fiebig, J. Phys. D **38**, R123 (2005).

[2] W. Eerenstein, N. D. Mathur, and J. F. Scott, Nature (London) **442**, 759 (2006).

[3] R. Ramesh and N. A. Spaldin, Nature Mater. **6**, 21 (2007).

[4] M. Weisheit, S. Fähler, A. Marty, Y. Souche, C. Poinsignon, and D. Givord, Science **315**, 349 (2007).

[5] W. Eerenstein, M. Wiora, J. L. Prieto, J. F. Scott, and N. D. Mathur, Nature Mater. **6**, 348 (2007).

[6] S. Sahoo, S. Polisetty, C.-G. Duan, S. S. Jaswal, E. Y. Tsymbal, and Ch. Binek, Phys. Rev. B **76**, 092108 (2007).

[7] C.-G. Duan, J. P. Velev, R. F. Sabirianov, W. N. Mei, S. S. Jaswal, and E. Y. Tsymbal, Appl. Phys. Lett. **92**, 122905 (2008).

[8] T. Maruyama, Y. Shiota, T. Nozaki, K. Ohta, N. Toda, M. Mizuguchi, A. A. Tulapurkar, T. Shinjo, M. Shiraishi, S. Mizukami, Y. Ando, and Y. Suzuki, Nat. Nanotechnol. **4**, 158 (2009).

[9] P. Borisov, A. Hochstrat, X. Chen, W. Kleemann, and Ch. Binek, Phys. Rev. Lett. **94**, 117203 (2005).

[10] V. Laukhin, V. Skumryev, X. Marti, D. Hrabovsky, F. Sanchez, M. V. Garcia-Cuenca, C. Ferrater, M. Varela, U. Luders, J. F. Bobo, and J. Fontcuberta, Phys. Rev. Lett. **97**, 227201 (2006).

[11] S. Heinze, X. Nie, S. Blügel, and M. Weinert, Chem. Phys. Lett. **315**, 167 (1999).

[12] M. Y. Zhuravlev, S. S. Jaswal, E. Y. Tsymbal, and R. F. Sabirianov, Appl. Phys. Lett. **87**, 222114 (2005).

[13] E. Y. Tsymbal and H. Kohlstedt, Science **313**, 181 (2006).

[14] M. Gajek, M. Bibes, S. Fusil, K. Bouzeouane, J. Fontcuberta, A. Barthelemy, and A. Fert, Nature Mater. **6**, 296 (2007).

[15] J. P. Velev, K. D. Belashchenko, D. A. Stewart, M. van Schilfgaarde, S. S. Jaswal, and E. Y. Tsymbal, Phys. Rev. Lett. **95**, 216601 (2005).

[16] J. P. Velev, C.-G. Duan, K. D. Belashchenko, S. S. Jaswal, and E. Y. Tsymbal, Phys. Rev. Lett. **98**, 137201 (2007).

[17] J. P. Velev, C.-G. Duan, J. D. Burton, A. Smogunov, M. K. Niranjan, E. Tosatti, S. S. Jaswal, and E. Y. Tsymbal, Nano Lett. **9**, 427 (2009).

[18] L. D. Landau and E. M. Lifshitz, *Classical Theory of Fields*, 4th ed. (Pergamon, Oxford, 1975).

[19] I. Dzyaloshinskii, Sov. Phys. JETP **10**, 628629 (1960).

[20] C.-W. Nan, M. I. Bichurin, S.-X. Dong, D. Viehland, and G. Srinivasan, J. Appl. Phys. **103**, 031101 (2008).

[21] H. Zheng, J. Wang, S. E. Lofland, Z. Ma, L. Mohaddes-Ardabili, T. Zhao, L. Salamanca-Riba, S. R. Shinde, S. B. Ogle, F. Bai, D. Viehland, Y. Jia, D. G. Schlom, M. Wuttig, A. Roytburd, and R. Ramesh, Science **303**, 661 (2004).

[22] F. Zavaliche, H. Zheng, L. M. Ardabili, S. Y. Yang, Q. Zhan, P. Shafer, E. Reilly, R. Chopdekar, Y. Jia, P. Wright, D. G. Schom, Y. Suzuki, and R. Ramesh, Nano Lett. **5**, 1793 (2005).

[23] D. Dale, A. Fleet, J. D. Brock, and Y. Suzuki, Appl. Phys. Lett. **82**, 3725 (2003).

[24] M. K. Lee, T. K. Nath, C. B. Eom, M. C. Smoak, and F. Tsui, Appl. Phys. Lett. **77**, 3547 (2000).

[25] R. V. Chopdekar and Y. Suzuki, Appl. Phys. Lett. **89**, 182506 (2006).

[26] C.-G. Duan, S. S. Jaswal, and E. Y. Tsymbal, Phys. Rev. Lett. **97**, 047201 (2006).

[27] K. Yamauchi, B. Sanyal, and S. Picozzia, Appl. Phys. Lett. **91**, 062506 (2007).

[28] M. K. Niranjan, J. P. Velev, C.-G. Duan, S. S. Jaswal, and E. Y. Tsymbal, Phys. Rev. B **78**, 104405 (2008).

[29] J. M. Rondinelli, M. Stengel, and N. A. Spaldin, Nat. Nanotechnol. **3**, 46 (2008).

[30] S. Zhang, Phys. Rev. Lett. **83**, 640 (1999).

[31] C.-G. Duan, J. P. Velev, R. F. Sabirianov, Z. Zhu, J. Chu, S. S. Jaswal, and E. Y. Tsymbal, Phys. Rev. Lett. **101**, 137201 (2008).

[32] R. A. de Groot, F. M. Mueller, P. G. van Engen, and K. H. J. Buschow, Phys. Rev. Lett. **50**, 2024 (1983).

[33] M. I. Katsnelson, V. Yu. Irkhin, L. Chioncel, A. I. Lichtenstein, and R. A. de Groot, Rev. Mod. Phys. **80**, 315 (2008).

[34] K. Schwarz, J. Phys. F: Met. Phys. **16**, L211 (1986).

[35] R. J. Soulen, Jr., J. M. Byers, M. S. Osofsky, B. Nadgorny, T. Ambrose, S. F. Cheng, P. R. Broussard, C. T. Tanaka, J. Nowak, J. S. Moodera, A. Barry, and J. M. D. Coey, Science **282**, 85 (1998).

[36] H. van Leuken and R. A. de Groot, Phys. Rev. B **51**, 7176 (1995).

[37] G. Kresse and D. Joubert, Phys. Rev. B **59**, 1758 (1999).

[38] The exchange-correlation potential is treated in the generalized gradient approximation (GGA). We use the energy cutoff of 500 eV for the plane-wave expansion of the PAWs and a $10\times10\times1$ Monkhorst-Pack grid for k-point sampling. Structural relaxations are performed allowing atomic movements along the z direction perpendicular to the film surface until the Hellman-Feynman forces become less than 1 meV/Å. A 12 Å vacuum layer is used to separate CrO_2 films in the supercell geometry.

[39] J. Neugebauer and M. Scheffler, Phys. Rev. B **46**, 16067 (1992).

[40] J. J. Attema, M. A. Uijttewaal, G. A. de Wijs, and R. A. de Groot, Phys. Rev. B **77**, 165109 (2008).

[41] The error in computation of α_S occurs mainly due to a finite mesh in the integration of the charge density resulting in the accuracy of about 1%.

[42] P. Schattschneider, S. Rubino, C. Hebert, J. Rusz, J. Kunes, P. Novak, E. Carlino, M. Fabrizioli, C. Panaccione, and G. Rossi, Nature (London) **441**, 486 (2006).